NEOPLASIA
www.neoplasia.com

Volume 20 Number 5 May 2018 pp. 478–488 478

# Combined Inhibition of ATR and WEE1 as a Novel Therapeutic Strategy in Triple-Negative Breast Cancer

Juan Jin[*,1], Hehui Fang[*,1], Fang Yang[*], Wenfei Ji[†], Nan Guan[‡], Zijia Sun[*], Yaqin Shi[*], Guohua Zhou[§] and Xiaoxiang Guan[*,f]

[*]Department of Medical Oncology, Jinling Hospital, Medical School of Nanjing University, Nanjing, China; [†]Department of Medical Oncology, Jinling Hospital, Medical School of Nanjing Medical University, Nanjing, China; [‡]International Department American Division, Nanjing Jinling High School, Nanjing, China; [§]Department of Pharmacology, Jinling Hospital, Medical School of Nanjing University, Nanjing, China

## Abstract

Triple negative breast cancer (TNBC) is a highly aggressive subtype of breast cancer that poses a clinical challenge. Thus, new therapy strategies are urgently needed. The selective WEE1 inhibitor, AZD1775, has shown strong anti-proliferative effects on a variety of tumors. Here, we first demonstrate that inhibition of ATR by selective inhibitor AZD6738 can enhance AZD1775-caused growth inhibition in TNBC. Our results show that the enhanced cell death is attributed to repressed DNA damage repair and excessive replication stress, thereby causing increased DNA damage reflected by accumulation of the DNA double-strand-break marker γH2AX. On the other hand, combined treatment with AZD6738 and AZD1775 forces mitotic entry of cells with DNA damages by activating CDK1 activity, inducing severely aberrant mitosis and mitotic catastrophe, ultimately resulting in cell death. Dual inhibition of WEE1 and ATR also inactivated RAD51-mediated homologous recombination, which sensitized TNBC cells to cisplatin and PARP inhibitor. Here, based on the preclinical results that ATR inhibition synergizes with WEE1 inhibition in TNBC, we propose that this combination therapy alone, or in parallel with chemotherapy, represents an innovative and potent targeted therapy in TNBC.

*Neoplasia (2018) 20, 478–488*

## Introduction

Triple negative breast cancer (TNBC), characterized by lacking estrogen receptor and progesterone receptor, as well as human epidermal growth factor receptor 2, has been a huge challenge due to the absence of endocrine therapy and effective target therapy. While conventional chemotherapy is the mainstay treatment of TNBC patients, toxicity with these agents is hard to tolerate, and improvement in prognosis of patients remains negligible. Accordingly, there is an urgent need for identification of novel cancer therapies for this malignant disease [1].

Although TNBC is characterized by high genetic complexity and a heterogeneous nature, it has been identified that most TNBCs are defective in DNA damage response (DDR), and over half of TNBCs harbor deficient p53 signaling, leading to an inactive G1/S checkpoint. Thereby, TNBC relies more on the G2/M checkpoint to respond to DNA damage [2–4].

Tyrosine kinase WEE1 plays a crucial role in the G2/M checkpoint and regulation of DNA synthesis during S phase by inhibiting the cyclin-dependent kinases CDK1/2. Destruction of the G2/M checkpoint by WEE1 inhibition will render cell apoptosis from accumulated DNA lesions and premature mitotic entry of cells [5]. Previous studies have found that WEE1 inactivation by siRNA or the WEE1 inhibitor AZD1775 in TNBC cells results in significantly increased level of γH2AX, a distinct marker of DNA double strand breaks (DSBs), S phase arrest and caspase-mediated cell death [6]. However, the discovery of how to exploit the potential and clinical utility of AZD1775 remains a high priority.

Coordinated and complex DDR is activated to cope with DNA damage, and the phosphatidylinositol 3-kinase-related kinase (PIKK) family members, ATM, ATR and DNA-PKcs, play essential roles in DDR. The ATM kinase particularly senses DSBs, phosphorylating CHK2, and subsequently inactivating CDC25c,

which reduces the CDK1 activity to prevent the cell cycle process and repair DNA damage [7]. ATR is activated by multiple DNA damage events and replication stress, subsequently activating its substrate CHK1. An increasing number of effector kinases associated with DNA replication stress, DDR and the cell cycle are substrates of the ATR-CHK1, including WEE1 and regulatory factors in the homologous recombination repair (HRR) pathway, such as BRCA1 and RAD51 [8]. DNA-PKcs can maintain genome stability under replication stress though phosphorylating the RPA32 on serine 4 and 8 [9]. DNA damage followed by WEE1 inhibition is suspected to activate the upstream DDR signal, and a series of related factors will be activated. Based on the above rationale, we tried to combine the WEE1 inhibitor with other agents targeting the DDR pathway to treat TNBC effectively. Although a close crosstalk between PIKK family members exists, substantial evidence shows that ATR seems to be more essential for cell survival compared to others [8]. Our data also found that the ATR inhibitor AZD6738 sensitized TNBC to the WEE1 inhibitor AZD1775 more significantly than inhibitors targeting other PIKK family members. More strikingly, a dramatic decrease in cell viability was observed following combination AZD6738 and AZD1775 treatment with cisplatin even in low concentrations, especially in BRCA1-deficient TNBC. We first elaborated the mechanisms of TNBC-special synthetic lethality utilizing ATR and WEE1 inhibitors in combination.

## Materials and Methods

### *Cell Culture and Cell Viability Assay*

The MDA-231, Hs578t, MDA-157, BT549, HCC1937, HCC70, MDA-468, MCF7 and MCF10A cell lines were purchased in 2016 to 2017 from the Chinese Academy of Science Committee Type Culture Collection Cell Bank (Shanghai, China). Authenticity of these cell lines was done by Chinese Academy of Science Committee Type Culture Collection Cell Bank before purchase by STR DNA typing methodology. MDA-231, MDA-157, BT549, HCC1937, HCC70 and MCF7 cells were grown in RPMI 1640 supplemented with 10% fetal bovine serum (FBS), Hs578t and MDA-468 cells were grown in DMEM supplemented with 10% FBS, MCF10A cells were grown in DMEM F12 supplemented with 5% horse serum, 1.4 lM cortisone, 10 lg/ml insulin, 100 ng/ml cholera toxin, and 20 ng/ml epidermal growth factor. All culture media contained 100 units/ml of penicillin and 100 units/ml of streptomycin and all cell lines were cultured at 37°C in a 5% CO2 atmosphere. For cell viability analysis, cells were plated in 96-well plates at 4,000 to 6,000 cells per well. The following day, cells were exposed to different concentrations of agents and after 72-hour exposure cell survival was assessed with the Cell Counting Kit-8 in accordance with the recommended guideline (KeyGEN Biotech, Nanjing, China). Combination index (CI) values, calculated using CompuSyn software (ComboSyn, Inc., NJ, USA).

### *Antibodies and Agents*

Antibodies against pATM S1981 (#5883), pATR S428 (#2853), pCHK1 S345 (#2348), pCHK2 T68 (#2197), pH2A.X S139 (γH2A) (#9718), pHH3 S10 (#9286), pCDC25c S216 (#4901), CDC25c (#4688), cleaved-caspase-3 (#9661), BRCA1 (#9010) and GAPDH (#2118), mouse IgG (#7076), rabbit IgG (#7074) were purchased from Cell Signaling Technologies; Anti-RAD51 (ab88572) from Abcam; Anti-pRPA32 (S4/S8) (A300-245A-T) from Bethyl Laboratories and PE-anti-pHH3 S10 (650807) and AlexaFluor488-anti-pH2A.X S139 was purchased by Biolegend. Antibodies were used at the manufacturer's recommended dilutions. Anti-rabbit IgG conjugated with FITC and Anti-rabbit IgG conjugated with FITC were purchased from Proteintech.

AZD1775 and AZD6738 were kindly provided by AstraZeneca Inc.; NU7441, KU-60019, Palbociclib, Roscovitine and Veliparib were obtained from MedChem Express; the above compounds were all diluted in DMSO. Cisplatin and Paclitaxel were purchased from Hansoh Pharmaceutical Co. (Jiangsu, China) and Zhejiang Haizheng Pharmaceuticals (Zhejiang, China), respectively.

### *Colony Forming Assays*

To assess effects on colony formation, cells were seeded at 400 cells/mL in 6-well plates. The following day, cells were exposed to inhibitors for 24 h, after which cells were washed with PBS then recovered in fresh medium for 10-14 days. Finally, cells were stained with crystal violet. Colonies containing ≥50 cells were counted.

### *siRNA Transfection and Lentivirus Transfection*

siRNAs targeting BRCA1 were transfected into cells using LipoFiterTM according to its protocol (HanHeng, Shanghai, China). Protein extracts and drug treatments were started 48 hours after transfection. siRNAs were obtained from Ruibo (Guangzhou, China).

In experiments analyzing exogenous BRCA1 mutation protein, we transduced cells with lentivirus encoding truncated variant of BRCA1 p.Trp372X ordered from GenePharma according to its guidance (Shanghai, China). After transfection for 72 h, cells were harvested for the next experiments.

### *Western Blot*

Cells after indicated treatment were washed three times with PBS and lysed in RIPA buffer containing protease and phosphatase inhibitor cocktails; Protein concentrations were determined with the BCA kit (All kits from KeyGEN Biotech, Nanjing, China). Western blot analysis was conducted using the above antibodies followed by immunoblotting as recently described [10].

### *Immunofluorescence*

MDA-231 or Hs578t cells were plated on eight-well chamber slides (Lab-Tek Products, Illinois, USA) and treated with agents the following day as described. After drug treatment, cells were stained according to immunofluorescence described before [11]. Mitotic and nuclear phenotypes of at least 100 cells per condition were assessed. Immunofluorescence images were obtained with a Zeiss Scope.A1.

### *Flow Cytometry*

Cells were incubated with culture medium in 6-well plates, and the following day cells were treated with the indicated drugs. For apoptosis and cell cycle analysis, the cells were treated as a previous document [12].

To detect DNA double-strand breaks, cells were fixed in precooled 4% paraformaldehyde overnight at 4°C, permeabilized with 0.1% Triton X-100 in PBS, incubated with antibody at its recommended concentration for 1 hour at room temperature. Samples were analyzed on a BD Calibur flow cytometer (BD Biosciences, CA, USA).

### *Xenograft Experiments and Tissue TUNEL Staining*

MDA-231 xenograft was established as previously described [13]. When tumor volume reached 100 $mm^3$ (±50), mice were randomized to four treatment groups (five animals in each group). The mice were treated with vehicle (orally), or AZD1775 at a dose of 30 mg/kg (in 0.5% methylcellulose) by oral gavage (p.o.), or AZD6738 at a dose of 60 mg/kg (in 10% DMSO, 40% propylene glycol, 50% dH2O) (p.o.), or both AZD1775 and AZD6738. The vehicle and drugs were administrated on days 0-4, 6-10.Tumors were measured once every three days and tumor volume was calculated as (width × length$^2$)/2. Tumors were taken 8 hours after last administration for western blot and immunofluorescence. Fixed tumors were performed with TUNEL Assay kit (KeyGEN Biotech, Nanjing, China) following the kit protocol.

### *Statistical Analysis*

All statistical tests were conducted with GraphPad Prism version 6.0. Data were analyzed using a Student's *t*-test. Data are presented as mean ± SD of three independent experiments unless stated otherwise. A $P$ value of $< .05$ was considered statistically significant. $^*P < .05$, or $^{**}P < .01$ or $^{***}P < .001$.

## Results

### *AZD6738 Potentiates AZD1775 Induced Anti-Proliferation Effect in TNBC*

AZD1775 is a potent and specific small-molecule inhibitor of WEE1, which has shown notable antitumor effects both as a monotherapy and in combination with chemotherapy in preclinical and clinical settings [14,15]. We first investigated the effects of AZD1775 (WEE1i) in a panel of TNBC cell lines. The data showed that TNBC cells were highly sensitive to AZD1775, as the majority of AZD1775 $IC_{50}$s in these cells were below 1 μM (Figure S1*A*).

To better understand the response following the AZD1775 treatment in TNBC, we determined the expression levels of several DDR molecules and pHH3, together with the cleaved apoptotic marker caspase-3 in MDA-231 and Hs578t by Western blot [5,14]. PCHK1 and pCHK2 are markers of ATR and ATM activation, respectively [8]. The results indicated that AZD1775 rapidly induced a time and dose dependent increase of γH2AX, pATR, pATM, pCHK1 and pCHK2 expression [16]. In addition, the results found that AZD1775 remarkably increased the level of pHH3, in as little as 1 hour, indicating an quick increase in the mitotic cells [5,14] (Figure 1*A*). Based on the above evidence that WEE1 inhibition induces serious DNA damage and activates the DDR pathway at the same time, we further investigated whether combining inhibitors targeting the DDR pathway with AZD1775 induced a synthetic lethality in TNBC. From the dose-response experiments, we found that the inhibition of ATR by AZD6738 (ATRi) [17] significantly enhanced the AZD1775-caused cell viability loss in TNBC cells, compared to the inhibition of ATM by KU-60019 (ATMi) [18] or DNA-PKcs by NU7441 (DNA-PKi) [19] (Figure 1*B*).

Most TNBC cells were also sensitive to AZD6738, a selective small molecule inhibitor of ATR that was recently introduced (Figure S1*B*). AZD6738 sensitized cells to AZD1775 in a dose-dependent manner in TNBC cells, and drug combination between AZD1775 and AZD6738 was markedly synergistic (Figures 1*C* and S1*C*) [20]. To further characterize the long-term effects of the combination, we examined the effects of AZD1775, AZD6738 or both in colony-forming assays. In MDA-231 and Hs578t, low concentrations of both single drugs had little effect on colony formation, but the same concentration of AZD1775 with 500 nM AZD6738 significantly inhibited colony formation. The CI vs. Fa plot showed that all CI values were <1 in TNBC cells (Figure 1*D*). Apoptosis assays also showed that the combined treatment triggered more significant cell apoptosis compared to AZD1775 or AZD6738 alone in MDA-231 and Hs578t (Figure 1*E*). In addition, we developed a subtype of AZD1775-resistant MDA-231 (MDA-231-R) cells and found that AZD6738 could sensitize the MDA-231-R to AZD1775 treatment (Figure S1*D*).

A previous study has demonstrated that the inhibition of WEE1 resulted in cell death in breast cancer cells, but not in the non-transformed MCF10A [6]. To extend our observations, we analyzed the interaction between AZD1775 and AZD6738 among the four cell lines using a fixed dose ratio model. We designed two combination ratios (1:5 and 5:1) and then calculated the CI values. The analysis revealed that the CI values at different inhibition levels in TNBC cells were all <1, while almost CI values in MCF7, a luminal A breast cancer cell line, and MCF10A, a breast epithelial cell line, were >1, demonstrating that there was no synergy of the drugs in the two cells (Figure 1*F*). The reason might be that p53 is mutated in MDA-231 and Hs578t, and yet is wild-type in MCF7 and MCF10A. DNA damage could activate p53-$p21^{Waf1/Cip1}$ pathway and then induced a distinct G1 arrest in MCF7 and MCF10A cells to repair the damage (Figure S1, and *E*). Furthermore, we found that the CI values among all the cells were smaller when the fixed concentration ratio was 1:5 (AZD1775: AZD6738), yielding better synergy (Figure 1*F*). The 1:5 dose ratio was closer to the ratio of $IC_{50\text{-}AZD1775}/IC_{50\text{-}AZD6738}$, which suggested that the optimal combination ratio is the equipotency ratio (e.g., $IC_{50\text{-}AZD1775}/IC_{50\text{-}AZD6738}$) in cells.

### *Combined ATR and WEE1 Inhibition Induces Excess DNA Damage and Replication Stress in TNBC Cells*

To address stress-induced DNA damage from various sources, CHK1 is phosphorylated by ATR at Ser345, and pCHK1 subsequently activates WEE1, maintaining CDK1 in its inactive Y15-phosphorylated form, which prevent cell cycle process and allow cells to repair DNA damage. The phosphatase CDC25c is supposed to dephosphorylate inhibitory phosphorylation of CDK1, driving cell cycle advance [8,16]. Furthermore, activated ATR-CHK1 and ATM-CHK2 signals phosphorylate CDC25c at Ser216, promoting CDC25c export into the cytoplasm, and thereby decreasing the level of CDC25c phosphatase in the nuclei [8,16]. Previous data and our results show that WEE1 inhibition can induce an increase of pCHK1 (Ser345) in a dose and time dependent manner [21] (Figures 1*A* and 2*A*). Western blot suggested that AZD6738 suppressed AZD1775-induced CHK1-Ser345 phosphorylation and increased γH2AX and cleaved caspase-3 expression in TNBC cells. The decrease of the pCHK1 (Ser345) level and limited increase of RAD51 protein implied the diminished DDR and hence induced more DNA damage and cell apoptosis. Compared to single-drug treatment, combinatorial treatment did not increase the pCDC25c (Ser216) protein level, indicating the highly activated CDK1 activity had a positive feedback effect, which inhibited the loss of its activator CDC25c (Figure 2*A*). The results of flow cytometry showed that the combined treatment triggered more significant DNA damage compared to AZD1775 or AZD6738 alone in MDA-231 and Hs578t (Figure 2*B*). Pan-nuclear γH2AX represents severe DNA damage and a pro-apoptotic signal [22]. Combination of AZD1775 and AZD6738 triggered a dose-dependent accumulation of γH2AX positivity, especially pan-nuclear γH2AX, in MDA-231 and Hs578t (Figures 2,

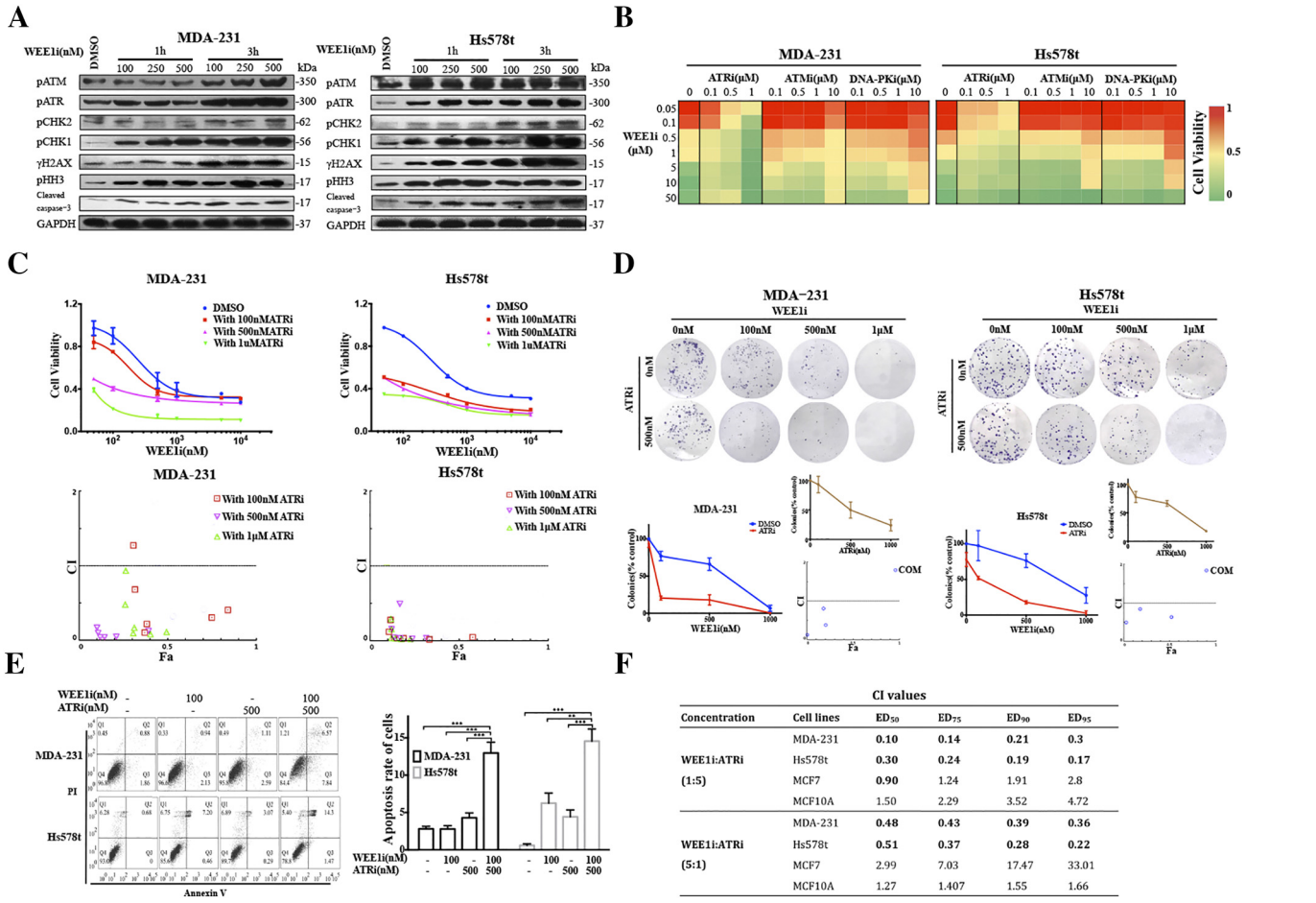


| Concentration | Cell lines | $ED_{50}$ | $ED_{75}$ | $ED_{90}$ | $ED_{95}$ |
|---|---|---|---|---|---|
| WEE1i:ATRi (1:5) | MDA-231 | **0.10** | **0.14** | **0.21** | **0.3** |
| | Hs578t | **0.30** | **0.24** | **0.19** | **0.17** |
| | MCF7 | **0.90** | 1.24 | 1.91 | 2.8 |
| | MCF10A | 1.50 | 2.29 | 3.52 | 4.72 |
| WEE1i:ATRi (5:1) | MDA-231 | **0.48** | **0.43** | **0.39** | **0.36** |
| | Hs578t | **0.51** | **0.37** | **0.28** | **0.22** |
| | MCF7 | 2.99 | 7.03 | 17.47 | 33.01 |
| | MCF10A | 1.27 | 1.407 | 1.55 | 1.66 |

**Figure 1. ATR inhibitor AZD6738 potentiates anti-proliferation of WEE1 inhibitor AZD1775 in TNBC cells. A,** MDA-231 and Hs578t cells were treated with 0.1-0.5 $\mu$M of AZD1775 for 1 and 3 h. Western blot showing activation of WEE1 targets. **B,** MDA-231 and Hs578t cells were treated with 0.05-50 $\mu$M of AZD1775 in combination with 0.1-10 $\mu$M of ATRi, ATMi or DNA-PKi for 72 h. Cell viability was detected by CCK8 (n = 3, mean). **C,** Proliferation curve of MDA-231 and Hs578t cells treated by 0.05-50 of $\mu$M AZD1775 with or without a constant dose of AZD6738 for 72 h (n = 3, mean ± SD) CI vs. Fa plot (combination index vs. fraction affected) for cell viability data presented in upper panel. The CI values were calculated by CompuSyn software. CI values below 1 are considered to have a synergistic interaction (n = 3, mean). **D,** Respective images of colony-forming results in MDA-231 and Hs578t treated by indicated concentrations of AZD1775 and AZD6738 (either single or both). Samples treated by inhibitors were compared to those of samples containing DMSO. In the upper small insets, the same cells were treated by the indicated concentrations of AZD6738. In the lower small insets, the CI values were calculated based on data in the main panel and upper inset (n = 3, mean ± SD). **E,** MDA-231 and Hs578t cells were treated for 24 hours with 100 nM of AZD1775, 500 nM of AZD6738 or both. Apoptotic cells were defined by flow cytometry with dual staining of annexin V (AV) and propidium iodide (PI) after treatment. Percentages of early (AV+PI−) and late (AV+PI+) apoptotic cells were calculated. Quantitative data of the apoptotic cells are shown (n = 3, mean ± SD) (**$P$ < .01 and ***$P$ < .001). **F,** Cells were treated with 0.1-50 $\mu$M of AZD1775 with AZD6738 for 72 h, and the dose ratio of AZD1775/AZD6738 was 1:5 or 5:1. Cell viability was investigated by CCK8 assay. The CI values at different inhibition levels (50%,75%,90% and 95%) analyzed by CompuSyn software are shown.

*C* and *D*; S2, *A* and *B*). Intriguingly, although the γH2AX level in the nuclei was seriously high after combination treatment, the level of nuclear RAD51 did not increase observably, indicating the unscheduled DDR (Figures 2*C* and S2*A*).

ATR inhibition can lead to the replication fork stalling, inevitably leading to excess single-stranded DNA (ssDNA) formation, which eventually induces DSBs [8]. Recently, WEE1 was also found to be implicated in response to replication stress, slowing cell cycle progression and stabilizing stalled DNA replication forks [23]. pRPA32 (S4/S8) is associated with ssDNA and is a specific marker of replication stress [9]. It was observed that although single drugs marginally increased the pRPA32(S4/S8)-positive cell population, the combinational drugs caused the extremely enhanced expression of pRPA32 (S4/S8), suggesting excessive ssDNA accumulation during prolonged S phase (Figures 2, *A*, *E* and *F*; S2*C*) [9].

### *Mitosis Catastrophe Caused by Forced Premature Mitosis of Cells With DNA Damage After Combined AZD1775 and AZD6738*

Western blot showed that co-treatment of AZD1775 and AZD6738 induced significant increase of pHH3, indicating the presence of numerous mitotic cells [5] (Figure 2*A*). We used a flow cytometer to investigate whether cells with DSBs were pushed into mitosis by probing cells with anti-pHH3 and anti-γH2AX antibodies. AZD1775 and AZD6738 in combination significantly increased the number of mitotic cells after 48 h treatment, and

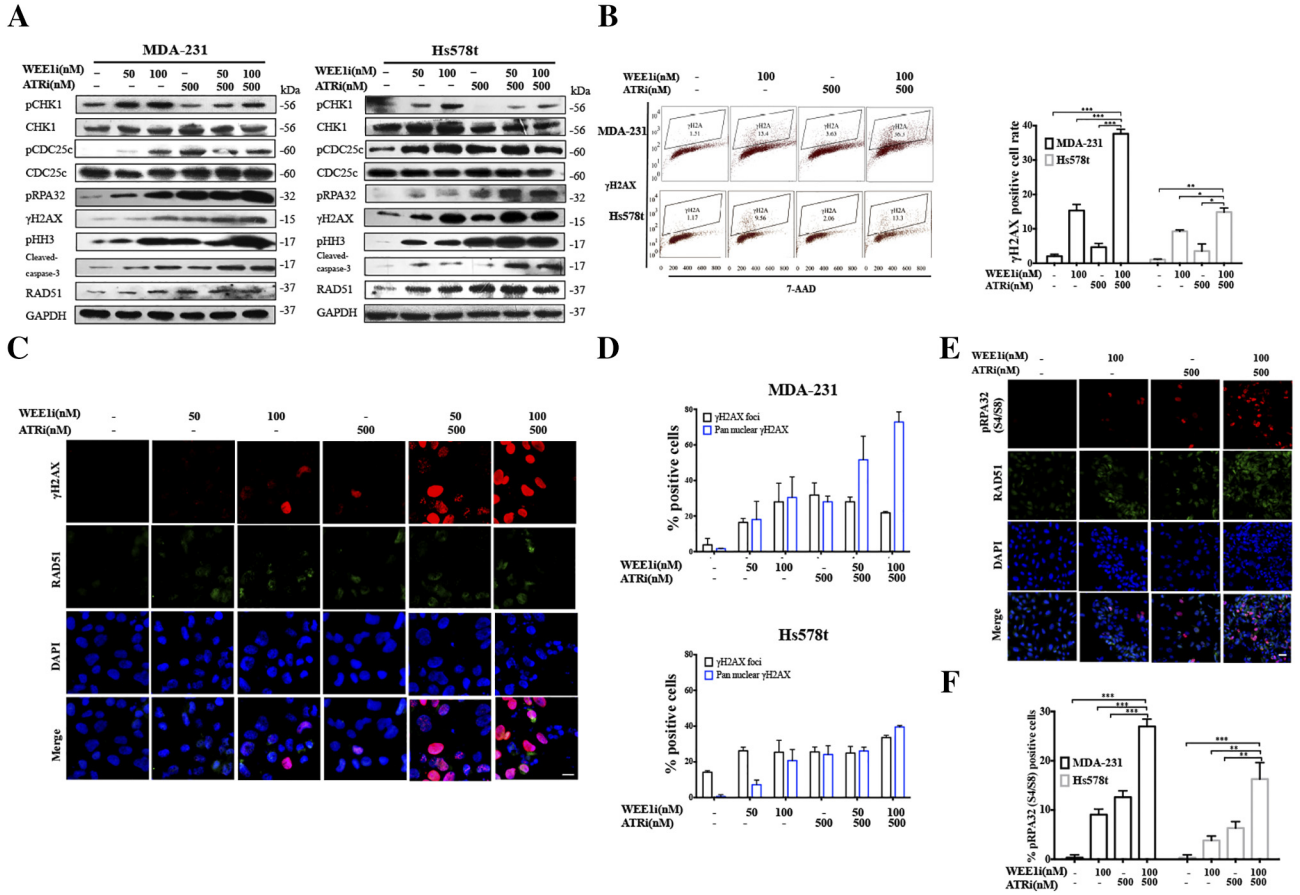


**Figure 2. AZD6738 targets DDR activated by AZD1775 and enhances AZD1775-induced replication stress in TNBC cancer cells. A,** MDA-231 or Hs578t cells were treated with 50 nM or 100 nM of AZD1775 with or without 500 nM of AZD6738 for 24 h. After treatment, western blot was performed using anti-γH2AX, anti-pCHK1 (S345), anti-CHK1, anti-pCDC25c (S216), anti-CDC25c, anti-pHH3, anti-RAD51 anti-pRPA32 (S4/S8), anti-cleaved-caspase 3, and anti-GAPDH antibodies. **B,** MDA-231 and Hs578t cells were treated for 24 hours with 100 nM of AZD1775, 500 nM of AZD6738 or both. Flow cytometry was used to identify the population of cells positive for γH2AX after treatment. Quantitative data of γH2AX-positive cell population are shown (n = 3, mean ± SD) (*$P$ < .05, **$P$ < .01, and ***$P$ < .001). **C,** MDA-231 cells were treated with 50 nM or 100 nM of AZD1775 with or without 500 nM of AZD6738 for 24 h. Cells were probed with anti-γH2AX and anti-RAD51 antibodies. Scale bar: 5 $\mu$m. **D,** Quantitative data of the γH2AX-positive (five or more foci per cell) cells and pan-nuclear γH2AX signal after indicated treatments in the MDA-231 and Hs578t cells are shown (n = 3, mean ± SD). **E,** MDA-231 cells were treated with AZD1775 or AZD6738 alone or in combination for 24 h. Nuclear expression of pRPA32 (S4/S8) was determined by immunofluorescent imaging. Scale bar: 10 $\mu$m. **F,** Quantitative data of pRPA32 (S4/S8) positive cells after the indicated treatments are shown in MDA-231 and Hs578t cells (n = 3, mean ± SD) (**$P$ < .01 and ***$P$ < .001).

notably almost all the pHH3-positive cells were γH2AX positive, indicating that the majority of mitotic cells harbored DNA damage (Figure 3*A*).

The existing DNA damage and forced mitotic entry perturbed the mitotic machinery. To directly observe the magnitude of abnormal mitoses, we examined microtubule organization during mitosis by double staining cells with anti-α-tubulin and anti-pHH3 antibodies. There was a striking increase in mitotic cells following combined exposure, in comparison with single-drug treatment (Figure 3, *B* and *D*). Additionally, immunofluorescence images showed that premature mitotic cells harbored multiple mitotic abnormalities, including but not limited to mono-or multi-polar spindles, disorganized spindles, centrosome clustering and cytokinesis failure (Figure 3, *C* and *D*). Aberrant mitotic machinery inevitably contributed to mitotic catastrophe and eventually cell death [24]. Those cells that slipped through the unscheduled mitosis had highly abnormal nuclear morphology characterized by gross micronuclei, which is a sign of genomic damage events and chromosomal instability [5] (Figure 3, *E* and *F*).

### *The Synergistic Cytotoxic Effect of Dual ATR and CHK1 Inhibition is Dependent on a CDK-Mediated Persistent Cell Cycle*

The CDK kinase family plays an essential role in cell cycle progression by regulating G1/S or G2/M transition. Current evidence demonstrates that CDK1, which triggers mitotic entry by binding cyclin B, is inactivated by WEE1. WEE1 phosphorylates its inhibitory phosphorylated site at Tyr15. Conversely, CDC25c phosphatase can cause the timely activation of CDK1 by dephosphorylating pCDK1 (Tyr15). When DNA is damaged, DDR blocks CDK1 activity to allow time for DNA damage repair through

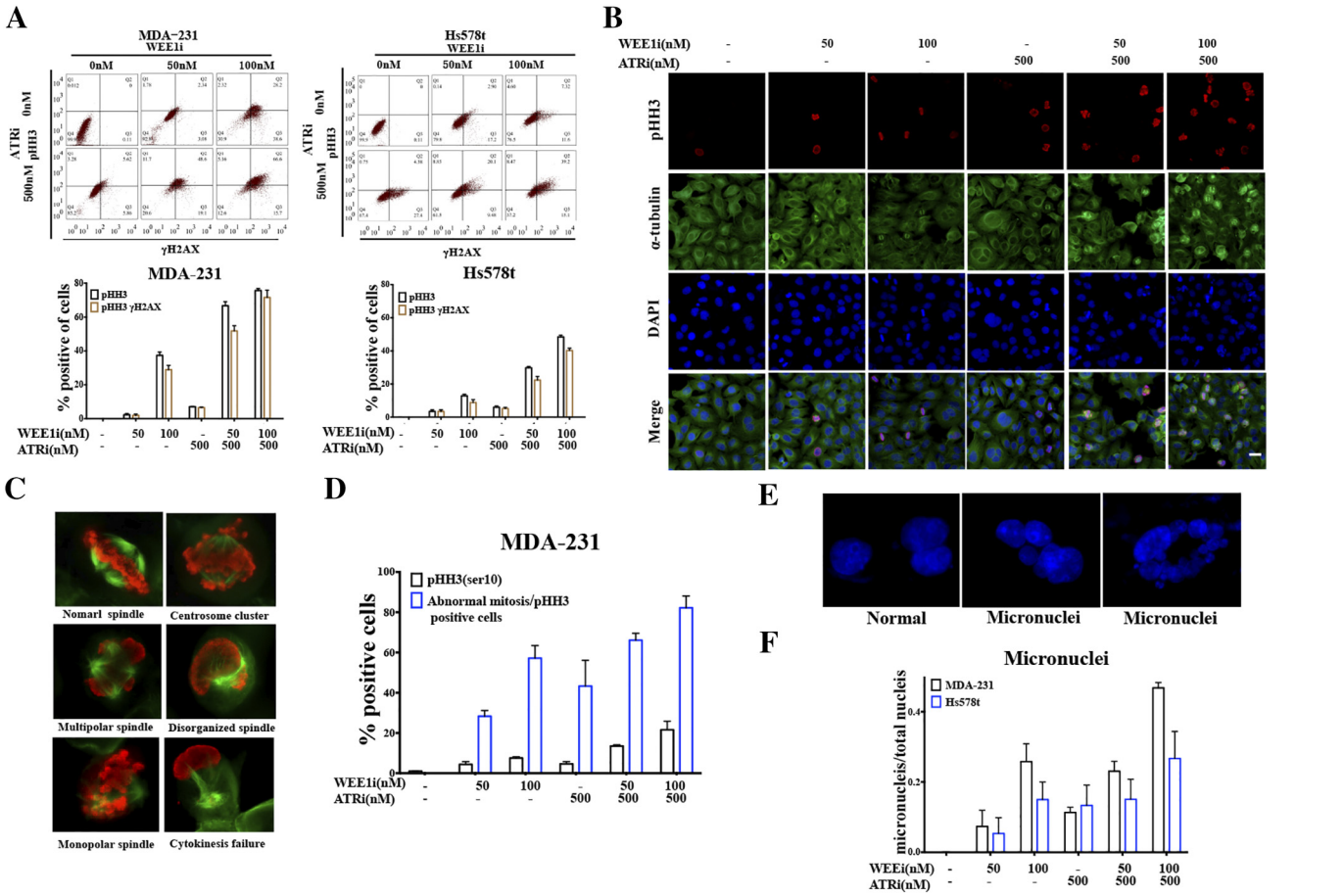


**Figure 3. Combined WEE1 and ATR inhibition forces mitotic entry of cells with DNA damage. A,** MDA-231 and Hs578t cells were treated with the indicated drugs for 48 h. Cells were probed with anti-pHH3 (Ser10) or γH2AX antibodies by flow cytometry. Quantitative data of flow cytometry in upper panel are shown (n = 2, mean ± SD). **B,** MDA-231 was co-treated with AZD1775 and AZD6738 for 24 h, followed by double staining for p-HH3 (red), or α-tubulin (green) together with DAPI (blue) by immunofluorescence. Scale bar: 10 μm. **C,** Respective images of typical mitotic phenotypes and several abnormal mitotic phenotypes in pHH3-positive MDA-231 cells are shown. Red, pHH3; green, α-tubulin. **D,** Quantification of pHH3-positive MDA-231 cells and abnormal mitotic cells in pHH3-positive MDA-231 cells after treatment for 24 h (n = 2, mean ± SD). **E,** Respective images of normal nuclei and micronuclei are shown. Blue, DAPI. **F,** Quantification of micronuclei numbers and total nucleuses in MDA-231 and Hs578t cells after treatment for 24 h (n = 2, mean ± SD).

phosphorylating CHK1 and CHK2 to activate WEE1 and inhibit CDC25c phosphatase [8,16,23]. Additionally, CDK2, CDK4 and CDK6 are important for the initiation of the cell cycle and the control of G1 to S phase transition [25]. A recent study identified S phase genes, including CDK2, CDK4 and CDK6, determined sensitivity of AZD1775 in cancer cells [26].

To test whether CDK activity was required for cytotoxicity induced by combined AZD1775 and AZD6738, MDA-231 and Hs578t cells were treated with DMSO, or the CDK1/2 inhibitor roscovitine (CDK1/2i), or the CDK4/6 inhibitor palbociclib (CDK4/6i), for 24 h, after which the CDK inhibitors were washed out and the cells were exposed to both AZD1775 and AZD6738 for 72 h. Cell viability results showed that roscovitine and palbociclib antagonized the cytotoxic effect of the combined treatment in TNBC cells (Figure 4*A*). Both CDK inhibitors rescued the accumulation of DNA damage induced by co-treatment (Figure 4, *B* and *C*). The constant ratio model also revealed that pretreated roscovitine and palbociclib increased the CI values, indicating that both inhibitors could abolish the synergetic effect of AZD1775 and AZD6738 (Table S1). Collectively, these results demonstrate that CDK activity is required for the synergy of the dual inhibition of WEE1 and ATR in TNBC cells.

### *Combination of WEE1 and ATR Inhibition Sensitizes TNBC Cells to Cisplatin Independent of BRCA Status*

Recent studies have implicated that both WEE1 and ATR are involved in HRR [8,23], and our findings also showed that, in spite of numerous DSBs induced by inhibition of WEE1 and ATR, the RAD51 level did not increase proportionally, indicating unscheduled HRR (Figure 2, *A, C* and *D*). Platinum salts, one of the most important agents in TNBC therapy, exert their anti-tumor activity by causing DSBs, which rely on HRR [27]. Therefore, we hypothesized that the combination of AZD1775 and AZD6738 might sensitize TNBC cells to platinum-based therapy. The CCK8 assays revealed that low doses of AZD1775 or AZD6738 did not enhance the effect of cisplatin in TNBC cells significantly, but dual exposure to both drugs lead to significant sensitivity to cisplatin (Figure 5*A*). Similar observations were also highlighted when cells were treated with veliparib, which is a PARP inhibitor targeting HRR (Figure S3*A*). To examine the potential mechanisms underlying these observations, cells were exposed to cisplatin with AZD1775, AZD6738 or both, and we found that inhibition of AZD1775 and AZD6738 strikingly repressed the cisplatin-induced RAD51 expression, resulting in more γH2AX accumulation and pushing more cells into mitosis

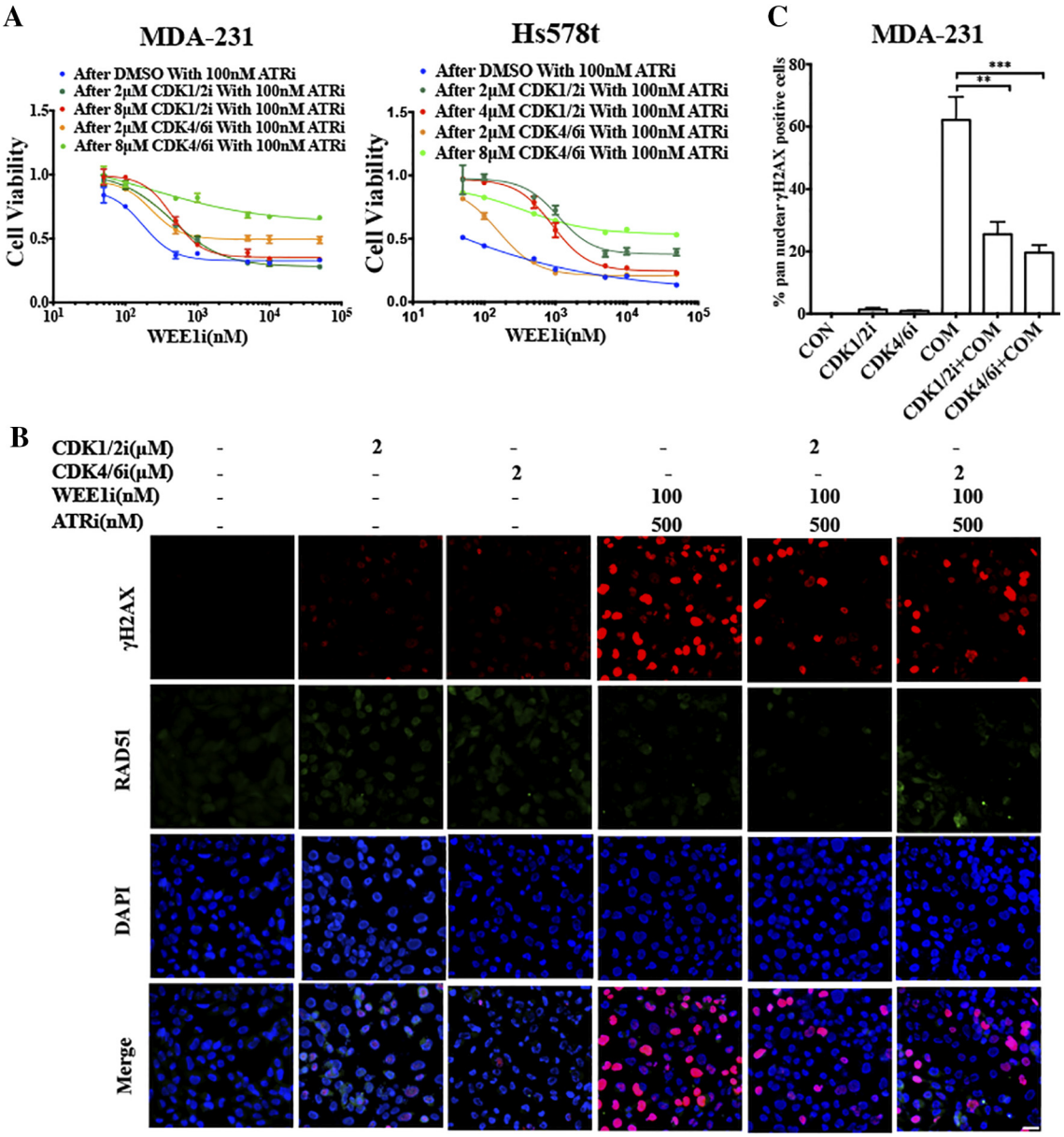


**Figure 4. CDK activities are required for the synergistic cytotoxic effect of combination treatment of AZD1775 and AZD6738 in MDA-231 and Hs578t cells. A,** MDA-231 and Hs578t cells were treated by DMSO, roscovitine (CDK1/2i), or palbociclib (CDK4/6i) for 24 h, after which DMSO and CDK inhibitors were washed out, and cells were treated with the indicated concentrations of AZD1775 with 100 nM of AZD6738 for another 72 h. Cell viability was detected by CCK8 (n = 3, mean ± SD). **B,** MDA-231 cells were pretreated with 2 $\mu$M of CDK1/2 inhibitor roscovitine, or 2 $\mu$M of CDK4/6 inhibitor palbociclib for 6 h before the medium was changed with that containing 100 nM of AZD1775 and 500 nM of AZD6738 for 24 h. Cells after treatment were probed with anti-γH2AX and anti-RAD51 antibodies and the respective images are shown. Scale bar: 10 $\mu$m. **C,** Quantitative data of the pan-nuclear γH2AX after treatment in Figure 4 *B* are presented (n = 2, mean ± SD) (**$P$ < .01 and ***$P$ < .001).

(Figures 5, *B–D* and S3*B*). In a parallel immunofluorescence analysis, nucleus images illustrated that the addition of AZD1775 and AZD6738 destroyed the co-localization of RAD51 and γH2AX signals in cells following treatment with cisplatin, and led to pan-nucleus γH2AX formation, revealing the unrepaired DNA damage (Figure 5*E*).

BRCA1 is a key protein in HRR, and notably, BRCA1-related abnormalities, including BRCA1 mutation and low BRCA1 mRNA expression, are strictly linked with TNBC [27]. We disabled BRCA1 by transfecting the cells with BRCA1 siRNA to investigate how BRCA1 impairment alone and in combination with AZD1775 or AZD6738 affected the response to cisplatin and veliparib in the BRCA1-wild type MDA-231 and Hs578t cells (Figure S3*C*). First, BRCA1 depletion did not sensitize the cells to AZD1775, but it did substantially sensitize the cells to the ATR inhibitor AZD6738 (Figure 5*F*). Therefore, we speculated that, compared to WEE1, ATR had a closer association with BRCA1-mediated HRR for cell survival. Second, disabled BRCA1 indeed sensitized MDA-231 cells to cisplatin and veliparib, which is consistent with earlier findings (Figures 5*G* and S3*D*). Third, a combination of AZD1775 and AZD6738 further sensitized BRCA1-deficient cells to cisplatin and veliparib, although this enhancement was smaller than that of control cells (Figures 5*G* and S3*D*). In addition, we observed a similar tendency

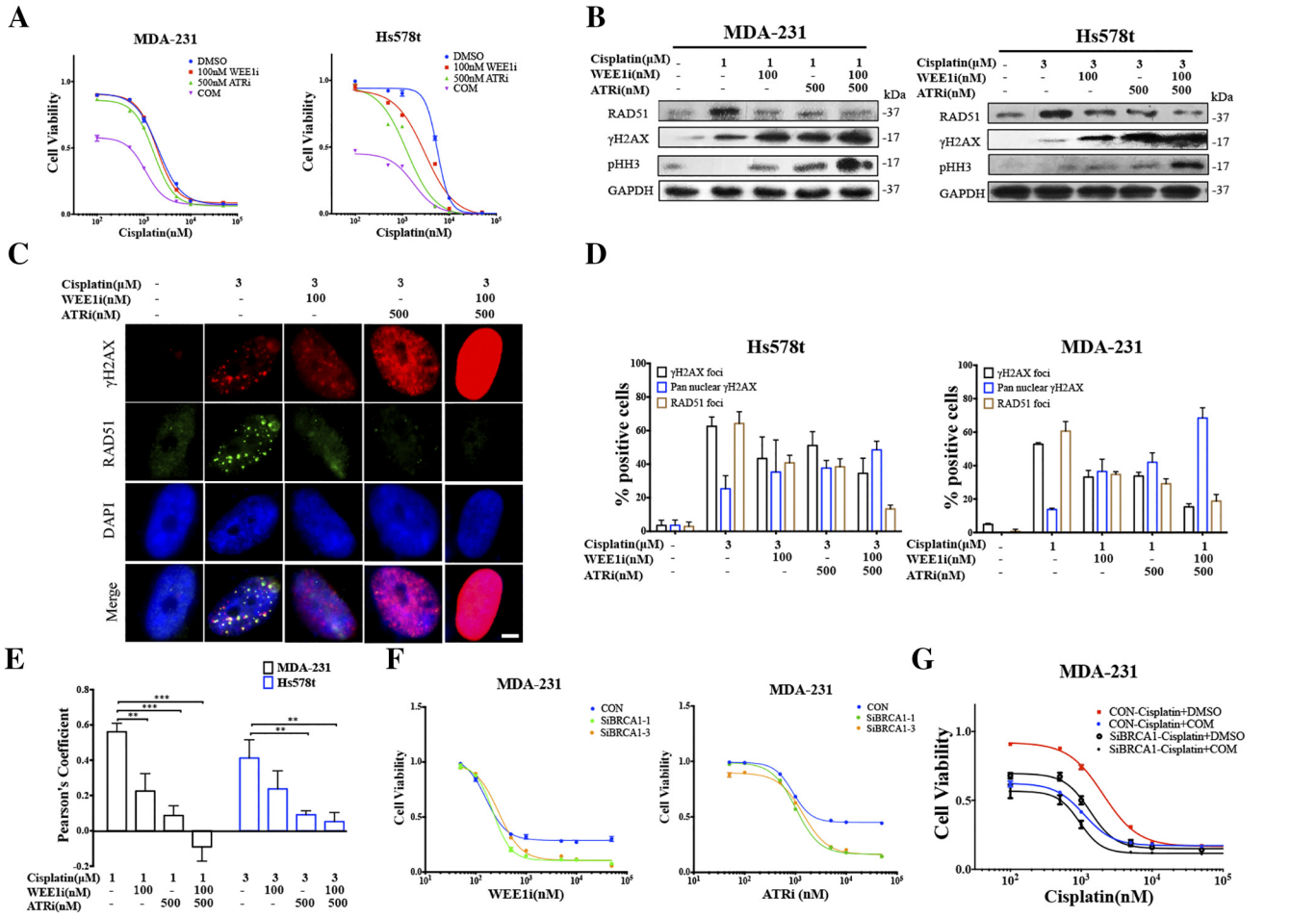


**Figure 5. Combined WEE1 and ATR inhibition further sensitizes TNBC cancer cells with defective HRR to cisplatin. A,** MDA-231 and Hs578t cells were treated for 72 h by the indicated concentrations of cisplatin with 100 nM of AZD1775, or 500 nM of AZD6738 or in combination. Cell viability was detected by CCK8 assay (n = 3, mean ± SD). **B,** Expression of RAD51, γH2AX and pHH3 of MDA-231 and Hs578t exposed to cisplatin alone, or in combination with AZD1775 or AZD6738, or both, were determined by immunoblot. **C,** An immunofluorescence assay was used to detect γH2AX and RAD51 expression in the nucleus in Hs578t following exposure to 3 $\mu$M of cisplatin with AZD1775 or AZD6738, or both. Scale bar: 2 $\mu$m. **D,** Percentage of cells with γH2AX foci (five or more foci per cell), pan-nuclear γH2AX signal or RAD51 foci (five or more foci per cell) after the indicated treatments in MDA-231 and Hs578t cells (n = 3, mean ± SD). **E,** Pearson's coefficient shown as the quantification of RAD51 and γH2AX co-localization of three separate experiments in Figure 5 *C* calculated by Image-Pro Plus software (n = 3, mean ± SD). **F,** After 48 h of treatment with vehicle or BRCA1 siRNA, MDA-231 cells were treated with the indicated concentrations of AZD1775 or AZD67398 for 72 h. Cell viability was analyzed by the CCK8 assay (n = 3, mean ± SD). **G,** Two days after the MDA-231 cells were transfected with vehicle or BRCA1 siRNA, cells were exposed to the indicated concentrations of cisplatin with or without the combination of 100 nM of AZD1775 and 500 nM of AZD6738 for 72 h, and cell viability was determined by CCK8 assay (n = 3, mean ± SD).

when MDA-231 cells were transfected with lentivirus encoding mutational BRCA1 (Figure S3*E*). Taken together, combinational AZD1775 and AZD6738 sensitized the TNBC cells to cisplatin and veliparib, independent of the BRCA status, and was demonstrated to further enhance the sensitivity in BRCA1-deficient TNBC cells, which highlights its clinical advantages in TNBC patients.

### *Co-effect of AZD1775 and AZD6738 on TNBC in Mouse Xenograft Models*

Next, we further explored the co-treatment of AZD1775 and AZD6738 in *vivo* using an MDA-231 xenograft model. Mice bearing MDA-231 xenografts were dosed with vehicle, 30 mg/kg of AZD1775 orally, 60 mg/kg of AZD6738 orally, or a combination on days 0-4 and 6-10. Combined treatment induced a significant reduction in tumor growth compared to single drug treatments (Figure 6*A*). Additionally, the single drug or combination treatments did not cause body weight loss (Figure 6*B*). The TUNEL results of the tumor tissues showed compared to the single drugs, combinational WEE1i and ATRi remarkably increased cell apoptosis (Figure 6, *C* and *D*). It was also confirmed that expression of γH2AX, pRPA32 (S4/S8) and pHH3 increased in the combination group (Figures 6*E* and S3*F*).

In conclusion, these data provide a combinational strategy in which the inhibition of both ATR and WEE1 induces an increase in CDK activity, ultimately leading to DNA damage, replication stress, mitotic catastrophe and finally, cell death (Figure 6*F*).

## Discussion

The vast majority of TNBC harbors p53 deficiency; therefore, TNBC is highly dependent on the G2 checkpoint mediated by WEE1, suggesting it is probably sensitive to the WEE1 inhibitor AZD1775, which we confirmed in seven TNBC cell lines [3] (Figure S1*A*). Our data show that the ATR inhibitor AZD6738 can sensitize

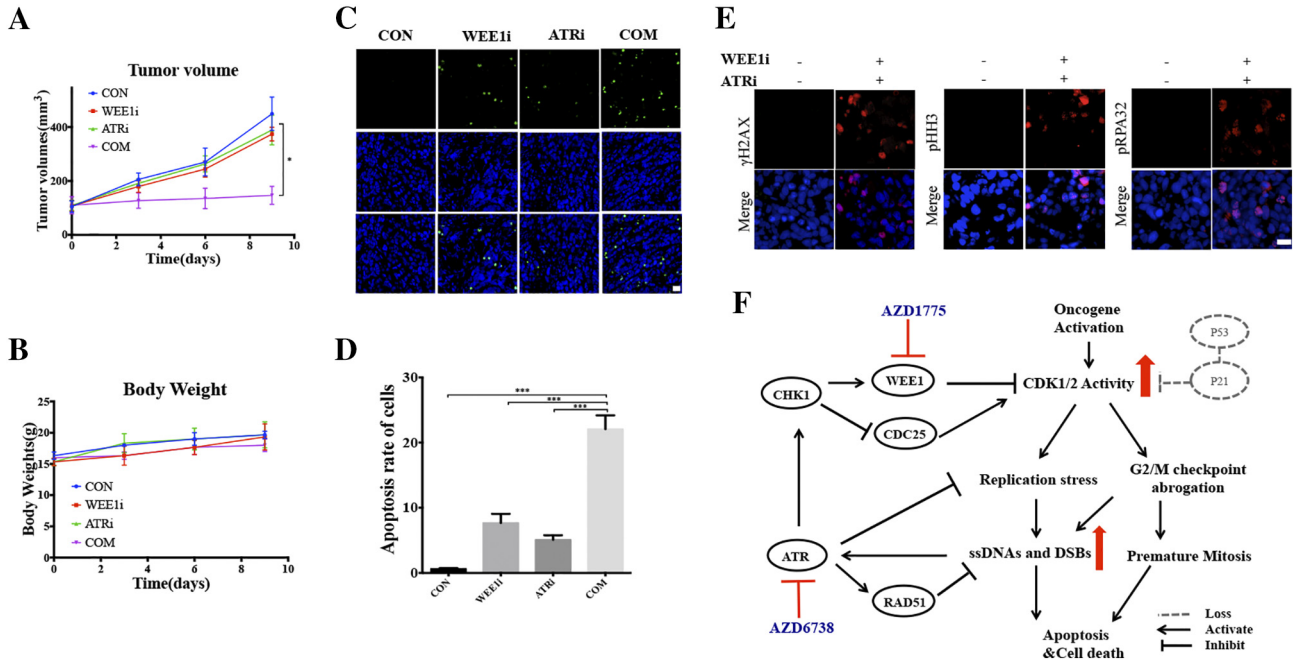


**Figure 6. In Vivo efficacy of AZD1775 and AZD6738.** Mice bearing MDA-231 xenografts with a tumor volume of 100±50mm$^3$ (6 for each group) were dosed with AZD1775 (WEE1i; 30mg/kg/d, p.o.) or AZD6738 (ATRi; 60 mg/kg/d, p.o.) or both. Vehicle and drugs were administered on days 0-4 and 6-10. Tumors were taken 8 hours after last drug administration for western blot and immunofluorescence assay. **A,** Tumor volumes were evaluated every 3 days and calculated by the formula:($S^2 \times L$) /2. S: short diameter; L: long diameter (*$P <$ .05). **B,** Body weight data for MDA-231 xenograft mouse. **C,** Apoptosis of the tumor tissues in different groups are shown by TUNEL assays. Scale bar: 20 $\mu$m. **D,** Quantification of apoptosis cells in different groups (n = 3, mean ± SD) (**$P <$ .01, and ***$P <$ .001). **E,** Immunofluorescence assay was utilized to analyze γH2AX, pRPA32(S4/S8) and pHH3 expression of tumor tissues from control group and combinational treatment group. Scale bar: 20 $\mu$m. **F,** Proposed mechanism for AZD1775/AZD6738 synthetic lethality in TNBC. WEE1 inhibition increases CDK1/2 activity, leading to replication stress and abrogation of G2/M checkpoint, which results in accumulated DNA damage including ssDNAs and DSBs. On the other hand, highly activated CDK1 activity forces cells with DNA damage into mitosis, triggering mitosis catastrophe. Replication stress and DNA damages activate ATR-CHK1 pathway, which activates WEE1 and inhibits CDC25c to inhibit CDK activity. Activated ATR also can directly regulate replication stress and DDR, which limits cytotoxic effect of AZD1775. AZD6738 inhibits ATR and thus enhances the forced mitosis and DNA damage, eventually leading to cell death. In almost all TNBC cells, the functions of p53/p21 are lost, resulting in unscheduled CDK activity that is more dependent on ATR-WEE1 pathway.

TNBC cells to the WEE1 inhibitor AZD1775 (Figure 1). Although WEE1 inhibitors and ATR inhibitors have shown single agent activity in various cancer types, our study demonstrates the synergy between the two kinds of inhibitors for the first time [8,23]. Interestingly, we observed that the co-effect of AZD1775 and AZD6738 did not exist in the luminal-A cell line MCF7 and the non-transformed MCF10A cell line, both of which have intact p53 function (Figure 1*E*). We postulated that the diminished co-effect was because of p53/p21 activation, but we could not rule out other possible mechanisms (Figure S1, and *E*).

AZD1775 can induce DNA damage, which activates ATR/ATM/DNA-PKcs and their substrates to repair damage independent of WEE1, countering the effects of AZD1775 [23]. However, weak enhancement of WEE1-induced cytotoxicity was observed when combined with the ATM or DNA-PK inhibitor compared to in combination with AZD6738 (Figure 1*B*). Our immunoblotting results also found that following AZD1775 treatment, pCHK1 (S345), which is a marker of activated ATR, increased in a time- and dose-dependent manner that was much more obvious than pCHK2 (T68), which is a marker of activated ATM (Figure 1*A*). This finding hinted that the ATR-mediated pathway played a more important role in AZD1775-induced DDR [16]. AZD6738 diminished ATR-mediated phosphorylation of CHK1 on Ser345, indicating that further DDR activation by ATR was suppressed (Figure 2*A*).

A study suggested that the combination of an ATR inhibitor and a CHK1 inhibitor induced an increase in CDK-mediated origin firing in cancer cells, ultimately resulting in replication catastrophe and cell death [28]. Our study also found that a synergistic effect of AZD1775 and AZD6738 required deregulated CDK activity (Figure 4). The functions of p53/p21 in preventing CDK activity in response to DNA damage are lost in p53-deficient TNBC cells, which makes these cells rely more on the balance of WEE1/CDC25c to regulate CDK activity [5]. Aarts et al. demonstrated the AZD1775 forced cells without complete DNA replication arrested in S-phase directly into mitosis, which was dependent on CDK1 activation, but not CDK2 [5]. Another study showed that down-regulated CDK2, but not CDK1, reduced the accumulation of γ-H2AX in WEE1-deficient osteosarcoma cells [26]. CDK2 mediates the replication origin during S phase and WEE1 inhibition is supposed to increase CDK2 activity, inducing uncontrolled replication fork and promoting more cells into S phase [29,30]. Based on the above evidences and our data, we hypothesize that following AZD1775 and AZD6738 treatment, highly activated CDK2 causes DNA damage during S phase and highly activated CDK1 pushes cells with DNA damage into mitosis (Figure 6*F*). Recently, a research indicated that the inactivation of G1/S regulatory genes, including CDK4 and CDK6, could nullify the anti-tumor effect of AZD1775 because DNA damage induced by AZD1775 occurred during S phase, and the cytotoxicity required

cells with DNA damage to go through S phase, which is in line with our data [26]. Conclusively, these studies show that highly amplified CDK activity drives cell progress inappropriately onward through the cell cycle without first coping with the DNA damage and proposes a caution that WEE1 and ATR inhibitors should not be combined with CDK inhibitors in the clinic.

Previous clinical trials have demonstrated that AZD1775 can enhance carboplatin efficacy in ovarian cancer [15]. However, our study observed AZD6738, not AZD1775 enhanced cisplatin efficacy in TNBC at low concentration. The possible reason was that ATR played a more key role in DDR after cisplatin-caused DNA damage. We widened the potential scope of AZD1775 and AZD6738 in TNBC, because combination of the low concentration of AZD1775 and AZD6738 enhanced cisplatin-induced cell death. Co-treatment further sensitized TNBC cells with disabled BRCA1 to cisplatin and thus clinical development will be further evaluated in BRCA-deficient tumors [31]. RAD51 is a critical component of the HRR, recruited to DSBs by BRCA2 and repairing the DSBs [32]. Combinational treatment decreased the RAD51 foci induced by cisplatin, which indicated that ATR/WEE1-regulated events were associated with the mobilization of the HRR machinery, but the exact mechanism needs further researches (Figure 5) [23,32].

In conclusion, we first identified the synergy between the WEE1 kinase inhibitor AZD1775 and the ATR kinase inhibitor AZD6738, which is a promising strategy for TNBC. We also postulate that the combinational strategy is potent in other malignant diseases, but further evidence is needed. Further research is warranted to find biomarkers that can be used in the selection of TNBC patients who will benefit from this therapy.

Supplementary data to this article can be found online at https://doi.org/10.1016/j.neo.2018.03.003.

## Author Contributions

Juan Jin designed research, performed research, analyzed data and wrote the paper; Hehui Fang performed research and analyzed data; Fang Yang, Wenfei Ji, Nan Guan, Yaqin Shi, Doudou Huang and Weiwei He performed research; Guohua Zhou gave advices; Xiaoxiang Guan designed the project

## Acknowledgements

We thank Astra Zeneca for AZD1775 and AZD6738 compounds and helpful advice. This research was supported by a Foundation for Clinical Medicine Science and Technology Special Project of the Jiangsu Province, China (No. BL2014071) (to XG), and National Natural Science Foundation of China (No. 81773102, No. 81470357).

## Conflict of Interest

The authors declare no conflict of interest.

## References

[1] Foulkes WD, Smith IE, and Reis-Filho JS (2010). Triple-negative breast cancer. *N Engl J Med* **363**, 1938–1948.

[2] Bado I, Nikolos F, Rajapaksa G, Gustafsson JA, and Thomas C (2016). ERbeta decreases the invasiveness of triple-negative breast cancer cells by regulating mutant p53 oncogenic function. *Oncotarget* **7**, 13599–13611.

[3] Turner N, Moretti E, Siclari O, Migliaccio I, Santarpia L, D'Incalci M, Piccolo S, Veronesi A, Zambelli A, and Del Sal G, et al (2013). Targeting triple negative breast cancer: is p53 the answer? *Cancer Treat Rev* **39**, 541–550.

[4] Yang F, Wang Y, Li Q, Cao L, Sun Z, Jin J, Fang H, Zhu A, Li Y, and Zhang W, et al (2017). Intratumor heterogeneity predicts metastasis of triple-negative breast cancer. *Carcinogenesis* **38**, 900–909.

[5] Aarts M, Sharpe R, Garcia-Murillas I, Gevensleben H, Hurd MS, Shumway SD, Toniatti C, Ashworth A, and Turner NC (2012). Forced mitotic entry of S-phase cells as a therapeutic strategy induced by inhibition of WEE1. *Cancer Discov* **2**, 524–539.

[6] Murrow LM, Garimella SV, Jones TL, Caplen NJ, and Lipkowitz S (2010). Identification of WEE1 as a potential molecular target in cancer cells by RNAi screening of the human tyrosine kinome. *Breast Cancer Res Treat* **122**, 347–357.

[7] Massey AJ (2016). Inhibition of ATR-dependent feedback activation of Chk1 sensitises cancer cells to Chk1 inhibitor monotherapy. *Cancer Lett* **383**, 41–52.

[8] Karnitz LM and Zou L (2015). Molecular Pathways: Targeting ATR in Cancer Therapy. *Clin Cancer Res* **21**, 4780–4785.

[9] Ashley AK, Shrivastav M, Nie J, Amerin C, Troksa K, Glanzer JG, Liu S, Opiyo SO, Dimitrova DD, and Le P, et al (2014). DNA-PK phosphorylation of RPA32 Ser4/Ser8 regulates replication stress checkpoint activation, fork restart, homologous recombination and mitotic catastrophe. *DNA Repair (Amst)* **21**, 131–139.

[10] Zhang W, Luo J, Yang F, Wang Y, Yin Y, Strom A, Gustafsson JÅ, and Guan X (2016). BRCA1 inhibits AR–mediated proliferation of breast cancer cells through the activation of SIRT1. *Sci Rep* **6**, 22034.

[11] Zhang W, Luo J, Chen F, Yang F, Song W, Zhu A, and Guan X (2015). BRCA1 regulates PIG3-mediated apoptosis in a p53-dependent manner. *Oncotarget* **6**, 7608–7618.

[12] Song W, Tang L, Xu Y, Xu J, Zhang W, Xie H, Wang S, and Guan X (2017). PARP inhibitor increases chemosensitivity by upregulating miR-664b-5p in BRCA1-mutated triple-negative breast cancer. *Sci Rep* **7**, 42319.

[13] Zhu A, Li Y, Song W, Xu Y, Yang F, Zhang W, Yin Y, and Guan X (2016). Antiproliferative Effect of Androgen Receptor Inhibition in Mesenchymal Stem-Like Triple-Negative Breast Cancer. *Cell Physiol Biochem* **38**, 1003–1014.

[14] Garimella SV, Rocca A, and Lipkowitz S (2012). WEE1 inhibition sensitizes basal breast cancer cells to TRAIL-induced apoptosis. *Mol Cancer Res* **10**, 75–85.

[15] Leijen S, van Geel RM, Pavlick AC, Tibes R, Rosen L, Razak AR, Lam R, Demuth T, Rose S, and Lee MA, et al (2016). Phase I Study Evaluating WEE1 Inhibitor AZD1775 As Monotherapy and in Combination With Gemcitabine, Cisplatin, or Carboplatin in Patients With Advanced Solid Tumors. *J Clin Oncol* **34**, 4371–4380.

[16] Ronco C, Martin AR, Demange L, and Benhida R (2017). ATM, ATR, CHK1, CHK2 and WEE1 inhibitors in cancer and cancer stem cells. *MedChemComm* **8**, 295–319.

[17] Jones CD, Blades K, Foote KM, Guichard SM, Jewsbury PJ, McGuire T, Nissink JW, Odedra R, Tam K, and Thommes P, et al (2013). Abstract 2348: Discovery of AZD6738, a potent and selective inhibitor with the potential to test the clinical efficacy of ATR kinase inhibition in cancer patients. *Cancer Res* **73**, 2348.

[18] Golding SE, Rosenberg E, Valerie N, Hussaini I, Frigerio M, Cockcroft XF, Chong WY, Hummersone M, Rigoreau L, and Menear KA, et al (2009). Improved ATM kinase inhibitor KU-60019 radiosensitizes glioma cells, compromises insulin, AKT and ERK prosurvival signaling, and inhibits migration and invasion. *Mol Cancer Ther* **8**, 2894–2902.

[19] Leahy JJ, Golding BT, Griffin RJ, Hardcastle IR, Richardson C, Rigoreau L, and Smith GC (2004). Identification of a highly potent and selective DNA-dependent protein kinase (DNA-PK) inhibitor (NU7441) by screening of chromenone libraries. *Bioorg Med Chem Lett* **14**, 6083–6087.

[20] Chou T-C (2006). Theoretical basis, experimental design, and computerized simulation of synergism and antagonism in drug combination studies. *Pharmacol Rev* **58**, 621–681.

[21] Guertin AD, Li J, Liu Y, Hurd MS, Schuller AG, Long B, Hirsch HA, Feldman I, Benita Y, and Toniatti C, et al (2013). Preclinical evaluation of the WEE1 inhibitor MK-1775 as single-agent anticancer therapy. *Mol Cancer Ther* **12**, 1442–1452.

[22] de Feraudy S, Revet I, Bezrookove V, Feeney L, and Cleaver JE (2010). A minority of foci or pan-nuclear apoptotic staining of gammaH2AX in the S phase after UV damage contain DNA double-strand breaks. *Proc Natl Acad Sci U S A* **107**, 6870–6875.

[23] Matheson CJ, Backos DS, and Reigan P (2016). Targeting WEE1 Kinase in Cancer. *Trends Pharmacol Sci* **37**, 872–881.

[24] Vitale I, Galluzzi L, Castedo M, and Kroemer G (2011). Mitotic catastrophe: a mechanism for avoiding genomic instability. *Nat Rev Mol Cell Biol* **12**, 385–392.

[25] Malumbres M and Barbacid M (2009). Cell cycle, CDKs and cancer: a changing paradigm. *Nat Rev Cancer* **9**, 153–166.

[26] Heijink AM, Blomen VA, Bisteau X, Degener F, Matsushita FY, Kaldis P, Foijer F, and van Vugt MA (2015). A haploid genetic screen identifies the G1/S

regulatory machinery as a determinant of Wee1 inhibitor sensitivity. *Proc Natl Acad Sci U S A* **112**, 15160–15165.

[27] Gerratana L, Fanotto V, Pelizzari G, Agostinetto E, and Puglisi F (2016). Do platinum salts fit all triple negative breast cancers? *Cancer Treat Rev* **48**, 34–41.

[28] Sanjiv K, Hagenkort A, Calderon-Montano JM, Koolmeister T, Reaper PM, Mortusewicz O, Jacques SA, Kuiper RV, Schultz N, and Scobie M, et al (2016). Cancer-Specific Synthetic Lethality between ATR and CHK1 Kinase Activities. *Cell Rep* **17**, 3407–3416.

[29] Hughes BT, Sidorova J, Swanger J, Monnat Jr RJ, and Clurman BE (2013). Essential role for Cdk2 inhibitory phosphorylation during replication stress revealed by a human Cdk2 knockin mutation. *Proc Natl Acad Sci U S A* **110**, 8954–8959.

[30] Petermann E, Woodcock M, and Helleday T (2010). Chk1 promotes replication fork progression by controlling replication initiation. *Proc Natl Acad Sci U S A* **107**, 16090–16095.

[31] Jin J, Zhang W, Ji W, Yang F, and Guan X (2017). Predictive biomarkers for triple negative breast cancer treated with platinum-based chemotherapy. *Cancer Biol Ther* **18**, 369–378.

[32] Kim H, George E, Ragland R, Rafial S, Zhang R, Krepler C, Morgan M, Herlyn M, Brown E, and Simpkins F (2017). Targeting the ATR/CHK1 Axis with PARP Inhibition Results in Tumor Regression in BRCA-Mutant Ovarian Cancer Models. *Clin Cancer Res* **23**, 3097–3108.